Quantitative Proteomics Analysis to Study the Protective Effects of Nerve Growth Factor on Hippocampal Mitochondria in VD Rats

Yanmei Zhang
Inner Mongolia People's Hospital
yuan yao (yuanyao129@imu.edu.cn)
Inner Mongolia People's Hospital https://orcid.org/0000-0002-0481-8286
Runxiu Zhu
Inner Mongolia People's Hospital
Niyang Aida
Inner Mongolia People's Hospital
Jun Yuan
Inner Mongolia People's Hospital
Wei Wu
Wenzhou Medical College Second Affiliated Hospital: Wenzhou Medical University Second Affiliated Hospital

Research Article

Keywords: Vascular dementia, nerve growth factor, hippocampal mitochondria, proteomics, rats

Posted Date: April 30th, 2021

DOI: https://doi.org/10.21203/rs.3.rs-456969/v1

Abstract

Background

Vascular dementia (VD) is a kind of clinical syndrome characterized with the impairment cognitive function caused by cerebrovascular disease. Genetics, biochemical, and morphological analyses of cell and animal models, reveal that mitochondria could have roles in this neurodegeneration.

Methods

We used Sprague-Dawley rats to establish VD model, and used the proteomics method based on relative quantification (iTRAQ) to identify the differentially expressed proteins in hippocampus mitochondria.

Results

A total of 33 differentially expressed proteins were identified between the VD rats and the VD rats treated with nerve growth factor groups. And five differentially expressed proteins (Rgs14, Slc7a14, Ppm1l, Kcnj10 and Syngr1) were identified after completing the sham-operate control, VD rats and VD rats treated with nerve growth factor groups, then successfully confirmed by western blot. Bioinformatics analysis suggested that the mitochondrial molecular mechanism of VD and the protective effect of nerve growth factor on mitochondrial function of VD rats may be due to different molecular mechanisms.

Conclusion

We estimated that mitochondrial dysfunction may be the onset of VD and key role in the pathological process of VD. This study not only has a deeper understanding of the mitochondrial molecular mechanism of VD, but also is helpful for the screening of drug targets.

Background

Vascular dementia (VD) is a kind of clinical syndrome characterized by cognitive impairment caused by cerebrovascular factors. At present, the objective reality of the medical profession is that with the progress of medical conditions and technology, the mortality rate of cerebrovascular diseases is decreasing year by year. However, the incidence of cognitive dysfunction due to cerebrovascular disease is gradually increasing. Therefore, it is of great significance to clarify the molecular mechanism of VD and provide reliable basis for the prevention and treatment of VD.

The pathological changes of VD involve the oxidative stress, mitochondrial lesions, abnormal genomic activity, synaptic dysfunction, protein metabolism disorders [1]. At present, the mechanisms about VD involve the cerebral ischemia and contradiction between supply and demand of oxygen metabolism exist

in neurons. The cerebral ischemia and hypoxia lead to oxidative stress and increase of free radicals in brain cells, which lead to mitochondrial dysfunction [2, 3]. Our previous studies also revealed abnormal expression of mitochondrial processing peptidase and mitochondrial precursor protein in the hippocampus of VD rats, suggesting that mitochondrial dysfunction functioned in the occurrence of neurodegenerative diseases [4].

It is well known that mitochondria are important organelles of human body. The position of mitochondria in nervous system is particularly important [5]. Neurons consume a lot of energy when they are active. When the oxidative phosphorylation process of mitochondria is impeded, neurons cannot start glycolysis as other types of cells to compensate [6]. In addition, the dynamic process of mitochondrial division and fusion is known as the differentiation and redistribution in synapses [7]. Mitochondrial dynamics and mitochon-drial transporting mechanisms ensure the long-distance transport and energy average distribution of mitochondria in neuronal endings. Abnormal mitochondrial fusion and division hinder the transport of mitochondria in neurons, resulting in the disorder of mitochondrial distribution and the decrease of energy metabolism efficiency [8]. Finally, through feedback, the cell signaling pathway is disturbed, which further leads to the degeneration of synaptic function and neuron death. Recent studies have also shown that mitochondrial dysfunction and fusion disorder can lead to degenerative diseases of the nervous system [9]. Therefore, abnormal mitochondrial fusion and division may be one of the key factors of dysfunction in mitochondria.

The nerve growth factor (NGF) can maintain the growth, development and reproduction of neurons [10]. NGF can promote neurite outgrowth in normal and ischemic brain regions and then slows down and prevents nerve cell apoptosis [11]. The experimental study of cerebral ischemia also shows that the combination of NGF and receptor can activate the injured nerve cells, help the recovery of the injured brain cells, regulate the metabolic function of nerve cells, improve the living environment of brain nerve cells, and effectively inhibit the death of brain cells [12]. Another proteomics study confirmed the different proteome in the VD cortex, using the iTRAQ-2D-LC–MS/MS strategy [13].

In our study, we used the samples from hippocampal brain area of VD rats with or without NGF intervention, to detect and identify the mitochondrial proteins with altered expression levels. The bioinformatics tools David and STRING were used to analyze dysfunctional proteins and determine if functional relationships would occur. This method can not only identify the protein sequence, but also quantify the related protein expression changes, which is helpful to quantify the potential biomarkers and better understand the pathology at the molecular level. The proteome reported in this paper also provided a reference data set for the basic research or translation research of VD in the future.

Methods

Animals and Ethics Statement

Adult male Sprague-Dawley rats (220±20g; No. 00010751; Experimental Animal Center, Wuhan First Hospital, Wuhan, Hubei Province, China; Laboratory animal facility license number: 00014834) were kept

in the laboratory with temperature of 22±2 ℃ and humidity of 65±2%, 4 rats per cage. Animals were fed in a 12 h light/dark cycle and were given food and water at will. All operations were performed in accordance with the guidelines approved by the Animal Care Committee of Inner Mongolia People's Hospital. We made every effort to relieve pain and discomfort.

Surgery procedure

The animals were weighed accurately and anesthetized by intraperitoneal injection of 10% chloral hydrate according to 0.3ml/100g. After intraperitoneal injection of chloral hydrate for 3-5 minutes, the righting reflex disappeared in animals. The animals were fixed on the operating table in supine position to ensure smooth breathing and disappeared with normal neck skin. The skin and subcutaneous tissue were cut through the middle of the neck, then the digastric muscle and sternocleidomastoid muscle were separated bluntly by tweezers. The carotid sheath was exposed. The bilateral common carotid artery and vagus nerve were separated carefully by glass needle, and the operation line 0 was inserted under the common carotid artery for reserve. Bilateral silk thread was drawn and bilateral common carotid artery of rats was clamped with non-invasive arterioles to block blood flow for 10 minutes, then removed and restored perfusion for 10 minutes for twice. Finally, the skin was sutured and the surgical site was disinfected. The gentamicin sulfate (0.2 ml) was injected intraperitoneally for anti-inflammation.

Groups

Animals were randomized into three groups (N=12 rats/group): (1) sham-operate control, SC, (2) the VD samples, VD, (3) the VD rats treated with NGF, VDN. A total 9 samples (n=3/each group) were performed the quantitative proteomics analysis and western bolt detection.

Preparation and detection of pathological specimens

Fresh brain tissue was fixed in 4 % paraformaldehyde and sectioned routinely. Mitochondria in hippocampus were labeled by Mito-Tracker GreenFM490/560, and morphological structure of mitochondria was observed by confocal laser microscopy.

2.5 Mitochondrial preparation

The isolated hippocampus was homogenated with glass homogenizer in the medium with ice residue. The mitochondria were extracted by differential centrifugation and gradient density centrifugation 10 times. The supernatant was centrifuged at 2000g for 3 minutes and repeated once; the supernatant was centrifuged at 12500g for 8 minutes and the supernatant was discarded; the precipitate was dissolved in 0.8ml 3% Ficoll medium and carefully spread on 3.2ml 6% Ficoll medium and centrifuged at 11050g for 30 minutes and the supernatant was discarded; the precipitate was suspended in the separation medium and centrifuged at 12500g for 8 minutes; finally, the precipitate was suspended with an appropriate amount of separation medium and the protein concentration was adjusted to a certain level About 10-20mg / ml. The protein concentration was determined by Lowry ` s method with bovine serum albumin as

the standard protein. Fresh mitochondrial suspension was taken to measure respiratory activity. All the above operations were completed at 0-4 ℃.

Hippocampal neuron staining

The hippocampal neuron of the sham-operate control, VD and VD rats treated with NGF groups were taken for 5 mm and fixed with 10 % neutral buffer at 4 ℃, then embedded with conventional wax blocks. Slice thickness was 5um. The slices were immersed in dimethylbenzene I, II and III of 90%, 80% and 70% concentration for 5 minutes. The slices were then immersed in 5g Nissl solution and soaked at 37 ℃ for 20 minutes. After incubation, the slices were washed with distilled water and then separated with 95% ethanol. Microscopically, there are obvious hippocampal neurons. The slices were dehydrated with anhydrous ethanol, transparent with xylene, and fixed with neutral rubber. Image analysis was carried out by using Image-Pro plus 4.5 software of Silver Spring Company in the United States to determine the cumulative integral optical density (IOD sum) and area value (area sum) of the positive product and calculate the average density (IOD / area)[14].

Extraction of total protein from mitochondrial cells in hippocampus

Total mitochondrial cell protein extraction and TMT quantitative proteomic experiment in hippocampus were commissioned by Majorbio Company in Shanghai. The instrument used was Triple TOF 5600 (AB Sciex, USA), and the analysis software was Proteinpilot (Applied Biosystems MDS Sciex, USA), Q-Exactive, EASY-nLC 1200, Orbitrap Fusion Tribrid (Thermo Fisher, USA) and Proteome Discoverer (Thermo Fisher, USA).

Total mitochondrial cell protein extraction

Samples were taken out under freezing condition and frozen on ice. The samples were added 10% SDS (Final concentration 1 %) and protease inhibitor PMSF (7.5 mM) to lyses for 30 minutes, and mixed every 5 minutes for 10 seconds. Protein supernatant was centrifuged at 12000g for 8 mins. BCA quantitative analysis was used, and then detected by SDS-PAGE. Protein was measured using the BCA method.

TMT Sample Preparation

Take 100 mg of above protein sample and supplement the volume with lysate to 100 μl. The final concentration of 10 mM TCEP was added and the reaction time was 60 min at 37 ℃. Add the iodoacetamide (40 mM) at room temperature for 40 minutes. Pre-cooled acetone (6:1 w/w) was added to each tube, and precipitated at -20℃ for 4 hours. The Protein samples were centrifuged at 10000g for 20 mins and then the precipitations were collected. The precipitations were dissolved with 100 μl TEAB (100 mM). Finally, the trypsin solution (1:50 w/w) was added for enzymatic hydrolysis at 37 ℃ overnight.

The above samples were labeled using an TMT reagent 10-plex protein quantitation kit (Thermo Fisher, USA) as follows: The sham-operate control was labeled with TMT10-130N, TMT10-130C and TMT10-131, and the VD samples were labeled with TMT10-128C, TMT10-129N and TMT10-129C, respectively;

the VD rats treated with NGF samples were labeled with TMT10-126, TMT10-127N and TMT10-128N, respectively.

High pH Reverse Phase Separation and Nano-LC–MS/MS Analysis

The Sep-Pack columns were used for desalination of TMT-labeled peptide mixtures. The high-pH reversed-phase column peptide fractionation kit (Thermo Fisher, USA) was used to classify the peptide fractions. A total of 10 distillates were charged according to the time. The distillates were concentrated by vacuum centrifugation and dissolved in a mass spectrometry sample buffer for the second dimensional analysis. Mass spectrometry parameters were set as follows: ion spray voltage of the inlet, 2.3 kV; mass spectra range, 350-1300 *m*/*z*; accumulation time per spectrum, 100 ms; and dynamic exclusion time, 18 s [15].

Proteomic Data Analysis and Bioinformatics

Proteomic data analysis and bioinformatics methods were described previously [15]. The Proteome Discoverer Software 2.1 (Thermo Fisher, USA), Protein pilot software (Applied Biosystems MDS Sciex) were used. All reported data were based on 95% confidence interval for protein and peptide identification as determined by Protein Pilot (Prot Score ≥1.3) [15]. Meanwhile, a cut off of 1% FDR (false discovery rate) and 40% isolation interference for peptide spectrum matches (PSMs) were required for all reported proteins. The Gene Ontology (GO) annotation was using the database (http://www.uniprot.org/uniprot/?query=organism:10116).

Verification of Differentially Expressed Proteins Using Western Blotting

Western blot was used to verify the quantitative proteomic results of TMT. The test method is described previously [16]. All the antibodies were diluted with 1:1000, and the secondary antibodies were diluted with 1:10000. The proteins were quantified by Image-J software. Each Western blot strip was measured three times and the average optical density was calculated.

Statistical Analysis

The data were expressed as mean ± SD. A Student' s *t* test in R language was used to calculate the *P* value of significant difference between samples. In this project, the screening criteria for significant difference expression proteins were: $P < 0.05$ & (FC<0.83 or FC>1.20).

Results

Identification of hippocampal neurons by Nissl staining

Under the light microscope, neurons stained blue could be seen. Rats in the sham-operate control group on Nissl staining section, the number of neurons was more and the color was dark. The dark blue is visible Nissl body, and the light blue was indicated the nucleus (Figure 1A). But in the same area in the VD

group, the number of neurons in dentate gyrus decreased and the staining was shallow. Nissl bodies were decreased or dissolved in cytoplasm, dendrites swelled and broken (Figure 1A). When the VD rats were treated with the nerve growth factor, the neurons started restocking and the color became more dark (Figure 1A). Furthermore, the mean density (IOD/AREA) was calculated and the results were consistent with the observation results (Figure 1B). The number of hippocampal neurons decreased, the Nissl body decreased or even disappeared, and the optical density decreased significantly. Because the light density was directly proportional to the color depth, it indicated that the neurons in this area become light stained. And, the color of neurons was determined by the number of Nissl bodies. In the absence of this substance in the cytoplasm, the light density decreased and the color became lighter.

TMT coupled with Nano-LC–MS/MS analysis of hippocampal mitochondria

Three hippocampal mitochondria were included in each group, and TMT proteomic analysis was carried out to identify different proteins that may be involved in the protection of NGF. The protein digestibility of the three samples was higher than 99%. The labeling efficiency was 95.9%. Through comparative analysis, 1572 proteins were identified as differentially expressed in the VD group *vs* sham-operate control group (Figure 2A, Table 1) and 1434 proteins were identified as differentially expressed in the VD rats treated with NGF group vs sham-operate control group (Figure 2B, Table 1). Similarly, the comparison between VD group and VD rats treated with NGF group showed that 17 proteins were up-regulated and 16 proteins were down regulated (Figure 2C, Table 1). And the GO annotation analysis showed that these proteins were major participants in cellular process, growth, response to stimulus, membrane part, metabolic process, multicellular organismal process and catalytic activity (Figure S1-S3). GO annotation analysis was used to classify these differentially expressed proteins according to cell composition, molecular function and biological process (Figure 3 A–C). As an example, the MS/MS spectrum and relative reported ion strength of abnormal expression protein A0A0G2K1G8 (slc7a14) were shown in Figure 4.

Analysis of differentially expressed protein by KEGG shown that the differentially expressed proteins were involved the following pathways: Endocytosis, Thermogenesis, Pathways in cancer, Huntington's disease, Protein processing in endocannabinoid signaling, Parkinson's disease and so on (Figure 5). After comparing the results Table 1, only five differentially expressed proteins were got including Rgs14, Slc7a14, Ppm1l, Kcnj10 and Syngr1 (Figure 6).

Western Blot Validation of Quantitative Proteomic Analysis

The next stage was to focus on the above five proteins, whose expressions were changed in three different comparisons (VD *vs* SC, VD *vs* VDN and VDN *vs* SC). From Figures 7A and 7B, we could see that the relative expression levels of Rgs14 was increased 2.1 fold in VD rats but significantly decreased in VD rats treated with NGF groups (1.5 fold) compared with the sham-operate control group. These results were consistent with the results based on iTRAQ (Figure 7C). In addition, the same comparison method was used to observe the relative expression levels of Ppm1l and Kcnj10, and we found that the levels of these two proteins were reduced in VD rats but raised in VD rats treated with NGF groups compared with

the sham-operate control group (Figure 7A and B). This part of the results could not correspond to the results based on iTRAQ (Figure 7C). The remaining two proteins Slc7a14 and Syngr1 showed the same trend in the expression levels, which were increased both in VD rats and VD rats treated with NGF groups compared with the sham-operate control group (Figure 7A and B). At the same time, it was consistent with the iTRAQ results.

Discussion

In this study, we have extracted total mitochondria in hippocampus and detected by technology iTRAQ and verified by western blot. Specifically, we identified several differentially expressed proteins of mitochondria in hippocampus neuros, to our knowledge this is the first report of the difference expression protein in mitochondria in hippocampus. We also observed the morphological changes of neurons. The data of proteomic study from Veen map revealed that the expression of five proteins have changed significantly, including regulator of G protein signaling 14 (Rgs14), solute carrier family 7 member 14 (Slc7a14) protein phosphatase Mg^{2+}/Mn^{2+}- dependent, IL (Ppm1l), ATP-sensitive inward rectifier potassium channel 10 (Kcnj10) and Synaptogyrin-1 (Syngr1). We also verified these proteins by western blot.

Specifically, the expression of Rgs14 present increased dramatically after interfered by NGF compared with control group, revealing Rgs14 has the striking regulation to the function of hippocampus mitochondria. Rgs14 is a kind of 60-kDa protein belonging to the RGS 12 family (R12) which is mainly expressed in the area CA2 of hippocampus pyramidal neurons and enriched post-synaptically in dendrites and spines in central nervous system [17–19]. Accumulating evidence has revealed that Rgs14 may negatively regulates the capacity of learning and memory in the CA2 region of the hippocampus by integrating G protein and ERK/MAPK signaling. [20–24] Furthermore, some researchers demonstrated Rgs14 knockout (KO) rats possess an unusually robust capacity for long-term potentiation (LTP) in CA2, which is absent in wild-type (WT) rats, and markedly enhanced spatial learning [19]. Taken together, these results show that Rgs14 acts as a critical factor for hippocampal based learning and memory and it belongs to a negative regulator. We have previously demonstrated Bilateral common carotid artery ligation (2-VO) could bring about the decline of capacity in spatial learning via Morris water maze on rats. And our current WB data showed the relative expression levels of Rgs14 VD rats and VD rats treated with NGF groups respectively are 2.1 and 1.5 compared with sham-operate control group, suggesting that NGF plays an important neuro-protection role. We assumed that the levels of Rgs14 might be specific increasing in VD rats, but partial recovery treated by NGF. This finding provides interesting clues towards the molecular mechanism about mitochondrial dysfunction simultaneously. We also inferred that Rgs14 proteins may be a kind of novel potential drug targets to dementia.

Similar to this protein are Ppm1l and Kcnj10. It was shown that Ppm1l inhibited inflammatory responses by directly dephosphorylating IKKβ and suppressing NF-κB activation in cardiac macrophages, subsequently prevented excessive scar formation and improved cardiac function [20]. Moreover, it was reported that Ppm1l was highly expressed in the central nervous system during mouse development and

played an important role in brain development [21]. To date, Ppm1l should be discovered and reported by proteomics techniques in mitochondrial hippocampus for the first time. Our findings established that Ppm1l expression of the mitochondrial hippocampus in VD was decreased significantly comparing with the sham-operate control group, whereas recovered after intervention by NGF (Fig. 7). We speculated Ppm1l was associated with the mitochondrial endoplasmic reticulum stress and displayed a lower expression in VD rats. But, the NGF could elevate the level of Ppm1l by promoting the growth, development, differentiation and maturity of central and peripheral neurons, maintaining the normal function of the nervous system, and accelerating the repair of the injured nervous system. Similarly, the NGF might elevate the level of Kcnj10 to protect the injured nervous system and there were few reports on the relationship between Kcnj10 and mitochondrial hippocampus.

With regard to Syngr1 and Slc7a14, the levels were found increased both in VD rats and VD rats treated with NGF groups. These results might indicate that Syngr1 and Slc7a14 played an important role in pathogenesis of vascular dementia, but the nerve growth factor did not affect the levels of these two proteins.

Conclusion

Proteomics analysis of the relative expression of mitochondrial proteins in hippocampus of Vascular dementia rats could find potential biological targets. Rgs14, Ppm1l and Kcnj10 might be good potential biological targets for drugs treating Vascular dementia. Nerve growth factor might be able to treat Vascular dementia.

Declarations

Ethics approval and consent to participate

This study was approved by the Animal Care Committee of Inner Mongolia People's Hospital.

Consent for publish

I give my consent for publication on behalf of all authors involved.

Availability of data and materials

All data, models, and code generated or used during the study appear in the submitted article.

Competing interests

The authors declare no competing interests in regards to this project.

Funding

This work was supported by grants from the National Natural Science Foundation of China (Grant No. 30960520 to Yanmei Zhang).

Author's Contribution

[#] These authors equally contributed to this work.

YZ and WW conceived and supervised the study; YZ and RZ designed experiments; NA and YY performed experiments; YZ provided new tools and reagents; YY and NA analysed data; YY, YZ and JY wrote the manuscript.

Acknowledgements

Not applicable.

Authors' information

Yanmei Zhang, Email: zhangyanmei2277@sina.com

Yuan Yao, Email: yuanyao129@imu.edu.cn

Runxiu Zhu, Email: zhurunxiu@163.com

Niyang Aida, Email: dnny6@sina.cn

Jun Yuan, Email: 13947108585@139.com

Wei Wu, Email: wuweiyjq74@163.com)

References

1. Prabakaran S, Swatton JE, Ryan MM, Huffaker SJ, Huang J-J, Griffin JL, Wayland M, Freeman T, Dudbridge F, Lilley KS, et al. Mitochondrial dysfunction in schizophrenia: evidence for compromised brain metabolism and oxidative stress. Mol Psych. 2004;9:684–97.
2. Hui L, Junjian Z. Cerebral hypoperfusion and cognitive impairment: the pathogenic role of vascular oxidative stress. Int J Neurosci. 2013;122:494–9.
3. Zu-Hang S, Qian C. Mitochondrial transport in neurons: impact on synaptic homeostasis and neurodegeneration. Nat Rev Neurosci. 2012;13:77.
4. Chen J, Zhou SN, Zhang YM, Feng YL, Wang S. Glycosides of cistanche improve learning and memory in the rat model of vascular dementia. Eur Rev Med Pharmaco. 2015;19:1234.
5. Saxton WM, Hollenbeck PJ: The axonal transport of mitochondria. J Cell Sci. 2012; 125:2095.
6. Mancuso M, Coppede F, Migliore L, Siciliano G, Murri L. Mitochondrial dysfunction, oxidative stress and neurodegeneration. J Alzheimers Dis. 2006;10:59–73.

7. Janikiewicz J, Szymański J, Malinska D, Patalas-Krawczyk P, Michalska B, Duszyński J, Giorgi C, Bonora M, Dobrzyn A, Wieckowski MR. Mitochondria-associated membranes in aging and senescence: structure, function, and dynamics. Cell Death Dis. 2018;9:332.
8. Zinsmaier KE, Babic M, Russo GJ. Mitochondrial transport dynamics in axons and dendrites. Berlin: Springer; 2009.
9. Okamoto KI, Hayashi Y, Sheng M. The Importance of Dendritic Mitochondria in the Morphogenesis and Plasticity of Spines and Synapses. Cell. 2004;119:873–87.
10. Bonini S, Aloe L, Bonini S, Rama P, Lamagna A, Lambiase A. Nerve Growth Factor (NGF): An Important Molecule for Trophism and Healing of the Ocular Surface. Oxygen Transport to Tissue XXXIII. 2002; 506:531–537.
11. Satoh T, Shingai R, Furuta K, Suzuki M, Watanabe Y. Neurite outgrowth-promoting prostaglandins that act as neuroprotective agents against brain ischemia and may enhance recovery of higher neuronal functions. Strategic Medical Science Against Brain Attack. 2002:78–93.
12. Gentry JJ, Casaccia-Bonnefil P, Carter BD. Nerve growth factor activation of nuclear factor kappaB through its p75 receptor is an anti-apoptotic signal in RN22 schwannoma cells. J Biol Chem. 2000;275:7558.
13. Datta A, Qian J, Chong R, Kalaria RN, Francis P, Lai MKP, Chen CP, Sze SK. Novel pathophysiological markers are revealed by iTRAQ-based quantitative clinical proteomics approach in vascular dementia. J Proteom. 2014;99:54–67.
14. Han Z, Chang Y, Zhou Y, Zhang H, Chen L, Zhang Y, Si J, Li L. GPER agonist G1 suppresses neuronal apoptosis mediated by endoplasmic reticulum stress after cerebral ischemia/reperfusion injury. J Neur Regen Res. 2019;14:1221.
15. Zhang P, Zhang L, Li Y, Zhu S, Zhao M, Ding S, Li J. Quantitative Proteomic Analysis To Identify Differentially Expressed Proteins in Myocardium of Epilepsy Using iTRAQ Coupled with Nano-LC–MS/MS. J Prot Res. 2018;17:305–14.
16. Zhang S, Wunier W, Yao Y, Morigen M. Defects in ribosome function delay the initiation of chromosome replication in Escherichia coli. J Bas Microbiol. 2018;58:1091–9.
17. Squires KE, Gerber KJ, Pare JF, Branch MR, Smith Y, Hepler JR. Regulator of G protein signaling 14 (RGS14) is expressed pre- and postsynaptically in neurons of hippocampus, basal ganglia, and amygdala of monkey and human brain. Brain Struct Funct. 2018;223:233–53.
18. Evans PR, Lee SE, Smith Y, Hepler JR. Postnatal developmental expression of regulator of G protein signaling 14 (RGS14) in the mouse brain. J Comp Neurol. 2014; 522.
19. Lee SE, Simons SB, Heldt SA, Zhao M, Schroeder JP, Vellano CP, Cowan DP, Ramineni S, Yates CK, Feng Y. RGS14 is a natural suppressor of both synaptic plasticity in CA2 neurons and hippocampal-based learning and memory. Proc Natl Acad Sci USA. 2010;107:16994–8.
20. Wang B. The roles of phosphotase PPM1L in inflammation and cardiac function after myocardial infarction and the. underlying mechanism Guangxi medical University; 2019.

21. Kusano R, Fujita K, Shinoda Y, Nagaura Y, Kiyonari H, Abe T, Watanabe T, Matsui Y, Fukaya M, Sakagami H. Targeted disruption of the mouse protein phosphatase ppm1l gene leads to structural abnormalities in the brain. Febs Lett. 2016; 590.

Tables

Table 1. Abnormal expression protein between groups.

Name	all_num	diff_num	up_num	down_num
VD_vs_VDN	5105	33	17	16
VDN_vs_SC	5105	1434	520	914
VD_vs_SC	5105	1572	579	993

Figures

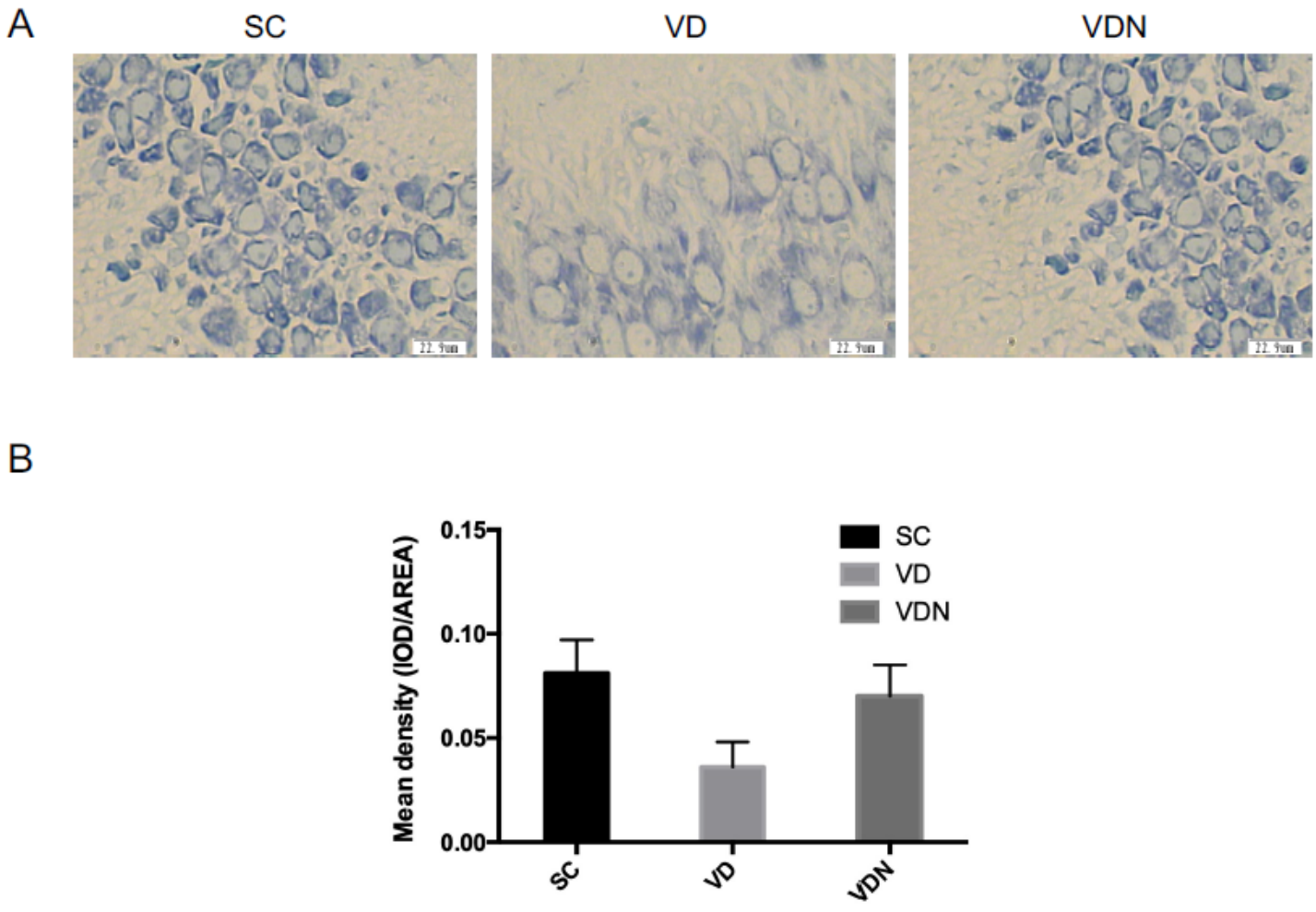

Figure 1

Identification of hippocampal neurons by Nissl staining. A. Nissl staining showing the hippocampus neurons in sham-operate control (SC), vascular dementia rats (VD) and VD rats treated with NGF (VND) groups. Bar=22.9 μm. B. The accumulative integral optical density (IOD SUM) and the area values (AREA SUM) were analyzed by Image-Pro Plus 4.5 software.

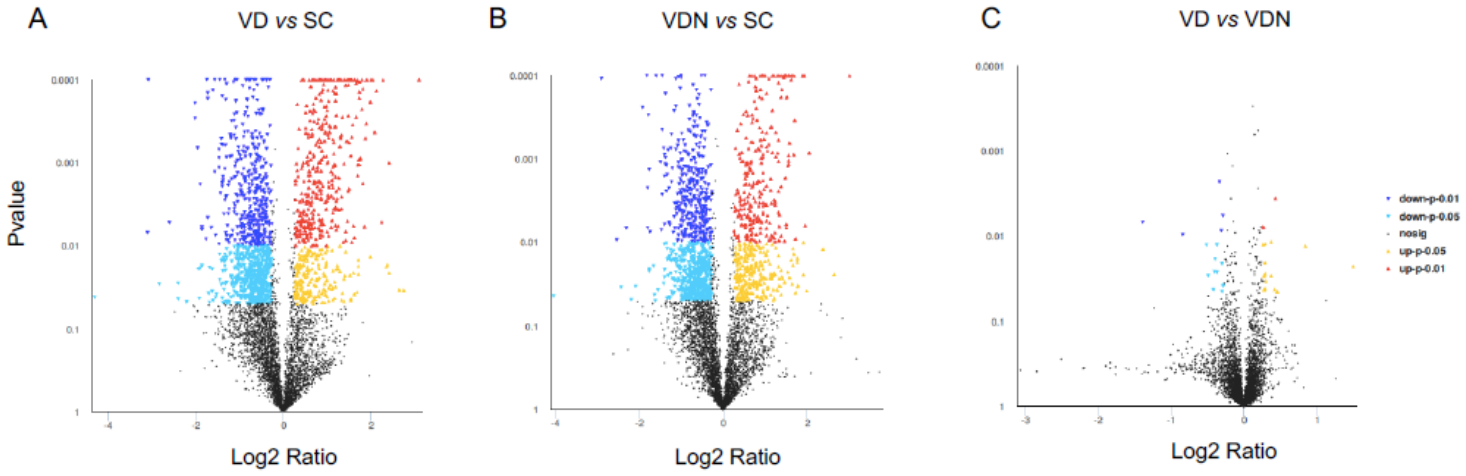

Figure 2

Differentially expressed proteins in hippocampal mitochondria of SC, VD and VDN groups. (A) Volcano plot of protein changes in hippocampal mitochondria of VD and acute SC groups. (B) Volcano plot of protein changes in hippocampal mitochondria of VDN and acute SC groups. (C) Volcano plot of protein changes in hippocampal mitochondria of VD and VDN groups. The screening criteria of significant difference expression protein was: P<0.05 &(FC<0.83 or FC>1.20). The abscissa in the figure is the multiple change value of the difference between the two samples, that is, the value obtained by dividing the expression quantity of sample 2 by the expression quantity of sample 1, which has been logarithmically processed.The ordinate is the statistical t-test p value of the difference in protein expression quantity, the smaller the p value, the more significant the expression difference. Each point in the figure represents a specific protein, the yellow point represents the protein significantly up regulated under P<0.05, the red point represents the protein significantly up regulated under P<0.01, the light blue point represents the protein significantly down regulated under P<0.05, the blue point represents the protein significantly down regulated under P<0.01, and the black point represents the protein with no significant difference. It can be seen that the point on the left is the protein with down-regulated differential expression, and the point on the right is the protein with up-regulated differential expression. The more points on the left, right and top are, the more significant the difference is.

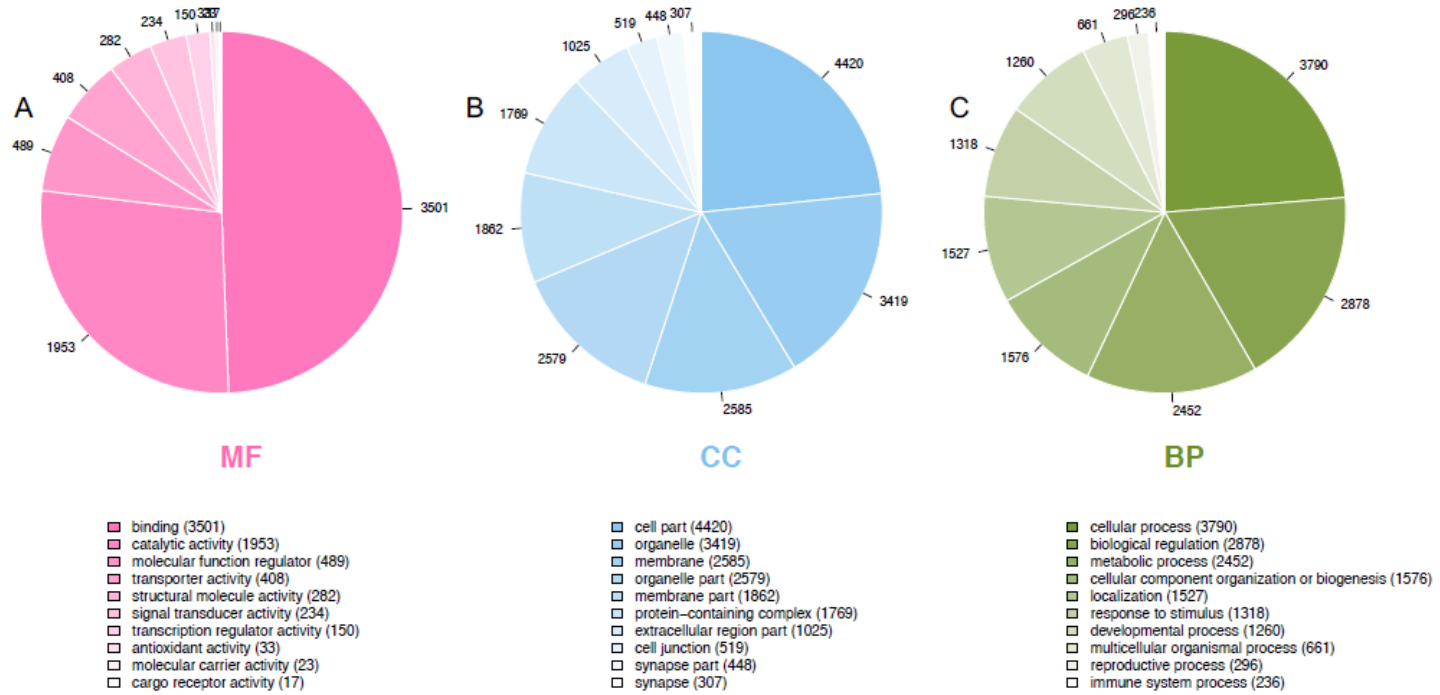

Figure 3

GO analysis of differentially expressed proteins using DAVID and Gene Ontology annotations. Different colors in each pie chart represent different GO terms, and the area represents the relative proportion of protein in the GO term. Three rows from left to right, which respectively represent the three branches of go, namely MF (molecular function, pink, A), CC (cell component, blue, B), BP (biological process, green, C). The figure below each row is annotated with the corresponding go classification terms.

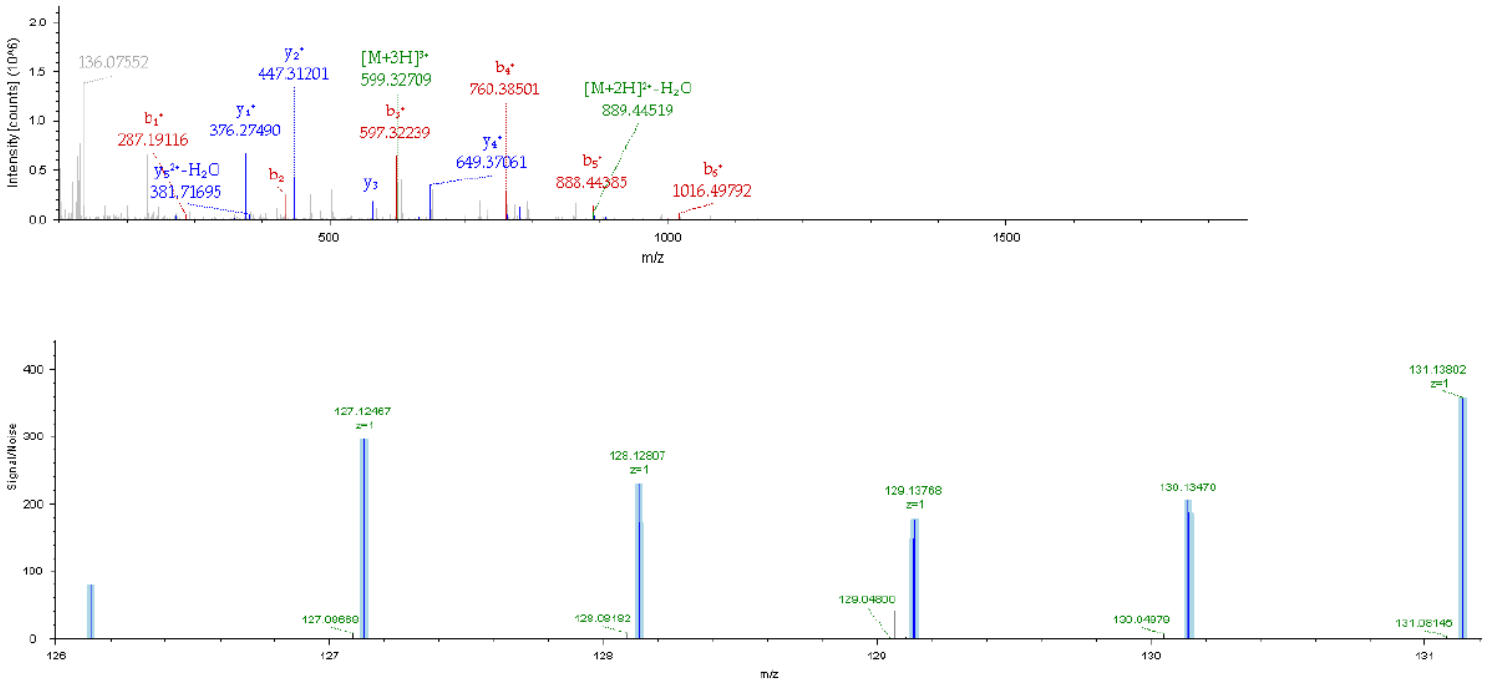

Figure 4

Example of one of differentially expressed proteins identified by iTRAQ coupled with nano-LC–MS/MS analysis. (A) MS/MS spectrum of A0A0G2K1G8 peptide (GFYYQQMSDAK) upregulated in VD and VDN groups. (B) Spectrum of relative reporter ion intensity for peptide.

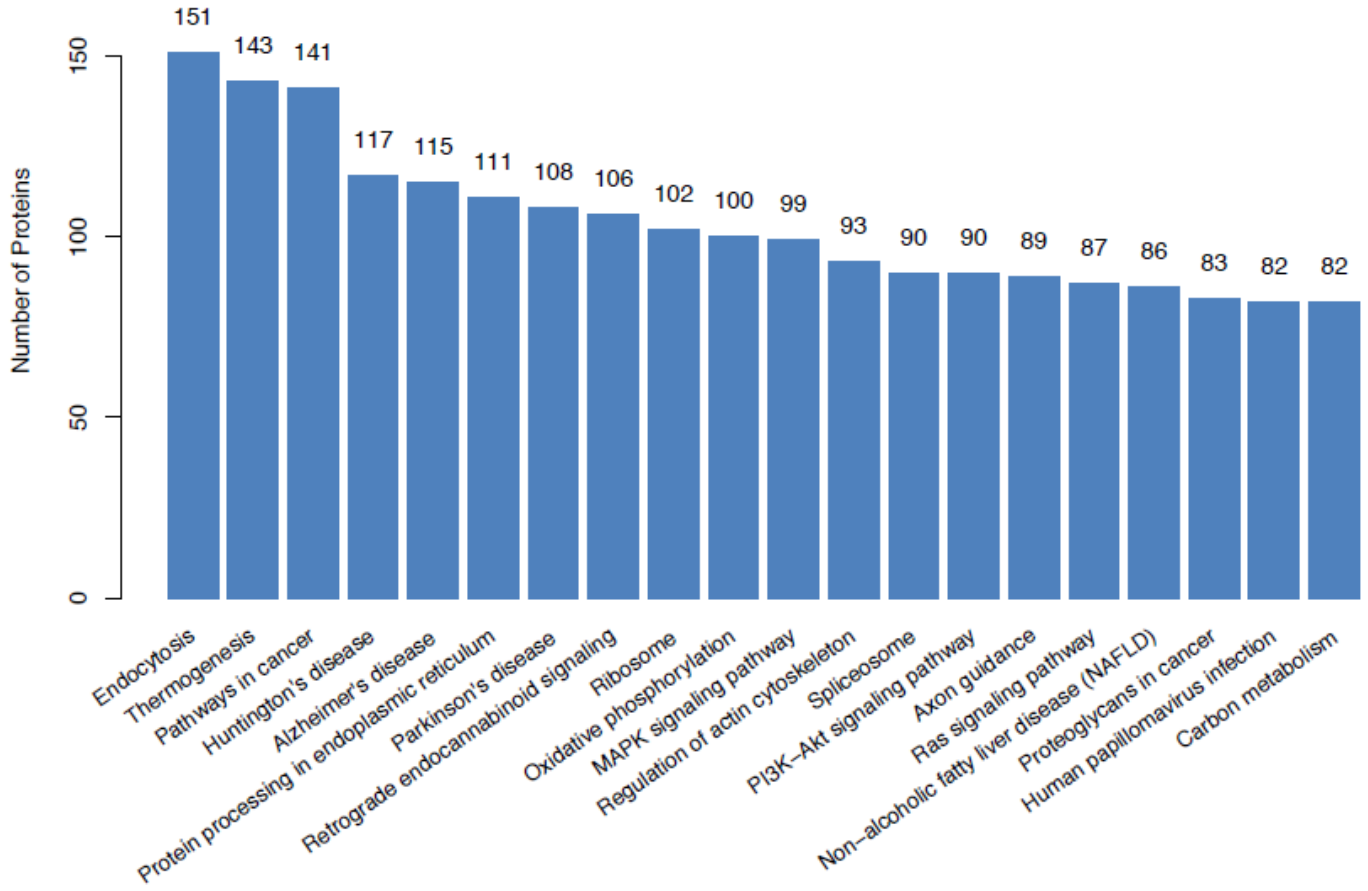

Figure 5

Top 20 pathways with the largest number of proteins. From left to right, it is arranged according to the number of protein contained from high to low. The higher the column is, the more active the biological pathway is in the measured sample.

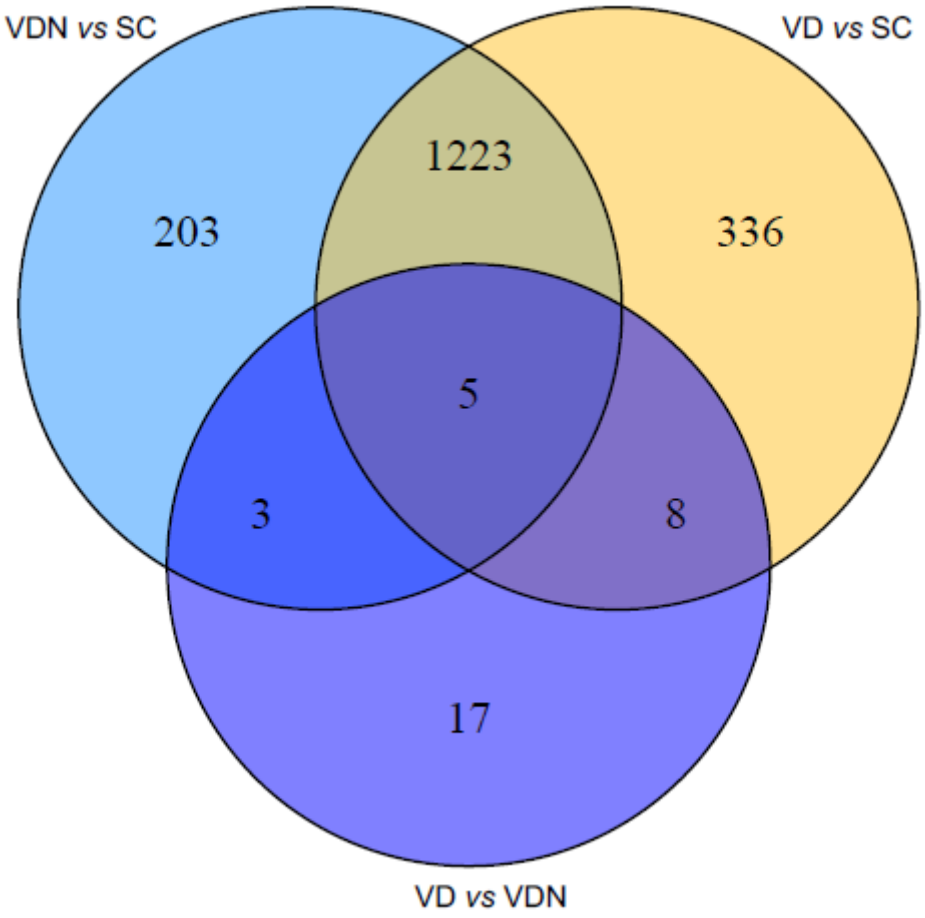

Figure 6

Differential proteins Veen map.

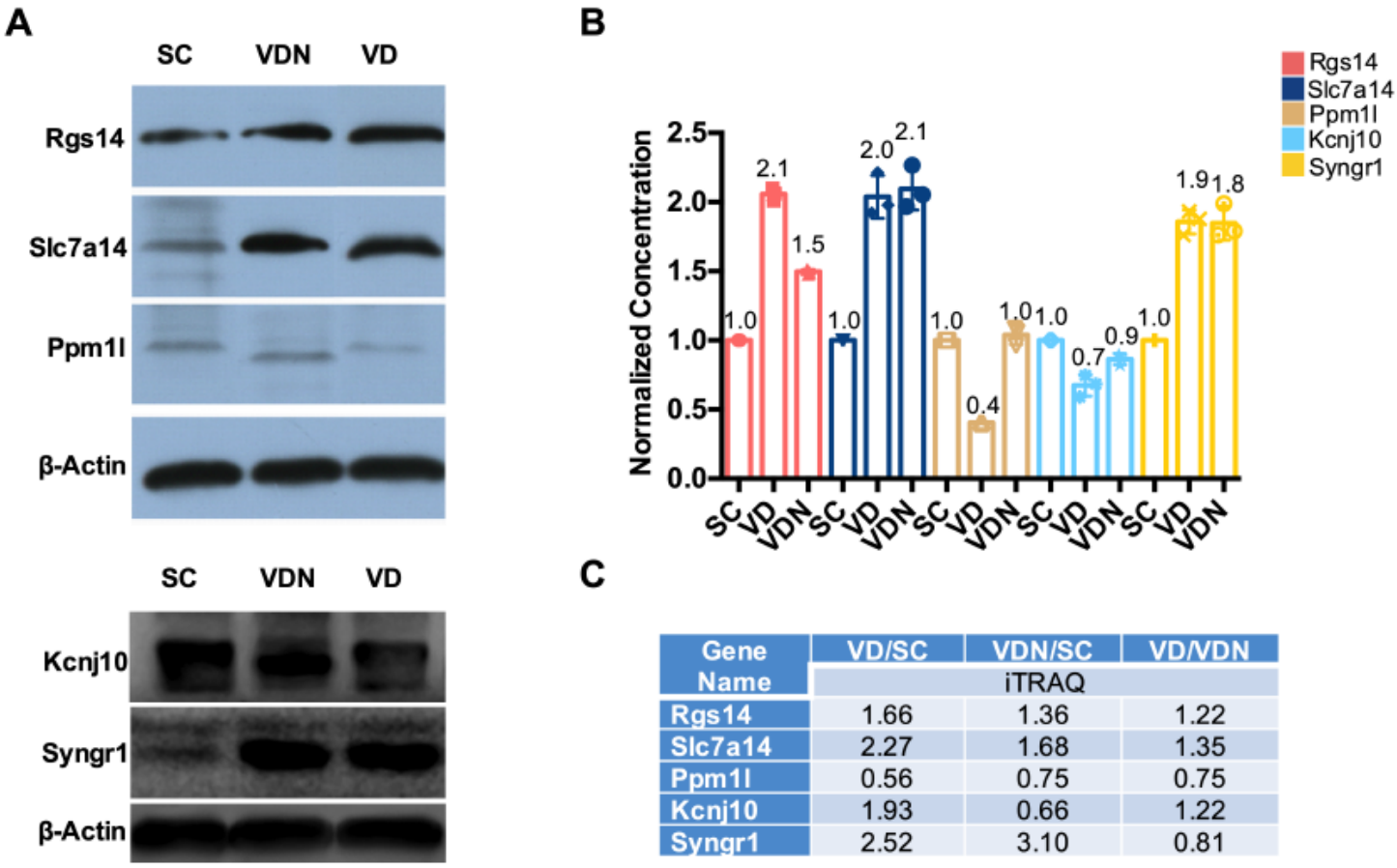

C

Gene Name	VD/SC	VDN/SC	VD/VDN
	iTRAQ		
Rgs14	1.66	1.36	1.22
Slc7a14	2.27	1.68	1.35
Ppm1l	0.56	0.75	0.75
Kcnj10	1.93	0.66	1.22
Syngr1	2.52	3.10	0.81

Figure 7

Western blot validation of Rgs14, Slc7a14, Ppm1l, Kcnj10 and Syngr1 identified by the iTRAQ-based proteomics approach. A and B. β-Actin was a loading control. Experiments were repeated three times. C. Differentially expressed proteins in hippocampal mitochondria in SC, VD and VDN groups Identified by iTRAQ based quantitative proteomics approach.

Supplementary Files

This is a list of supplementary files associated with this preprint. Click to download.

- FigureS13.pdf